Journal of Alloys and Compounds 509 (2011) 5974–5980

Contents lists available at ScienceDirect

Journal of Alloys and Compounds

journal homepage: www.elsevier.com/locate/jallcom

Characterization of alkaline-earth oxide additions to the MnO_2 cathode in an aqueous secondary battery

Manickam Minakshi [a,*], Mark Blackford [b], Mihail Ionescu [c]

[a] Extractive Metallurgy, Murdoch University, Murdoch, WA 6150, Australia
[b] Institute of Materials Engineering, ANSTO, Lucas Heights, NSW 2234, Australia
[c] Institute for Environment Research, ANSTO, Lucas Heights, NSW 2234, Australia

ARTICLE INFO

Article history:
Received 28 December 2010
Received in revised form 28 February 2011
Accepted 6 March 2011
Available online 11 March 2011

Keywords:
Aqueous battery
Manganese dioxide
Alkaline-earth oxide
Hetaerolite

ABSTRACT

The effect of alkaline-earth oxide additions on aqueous rechargeable battery is investigated using microscopic and spectroscopic techniques. The alkaline-earth oxide additions such as magnesium oxide (MgO) and barium oxide (BaO) were physically mixed to the manganese dioxide (MnO_2) cathode of a cell comprising zinc as an anode and aqueous lithium hydroxide as the electrolyte. The results showed that such additions greatly improved the discharge capacity of the battery (from 145 to 195 for MgO and 265 mAh/g for BaO). Capacity fade with subsequent cycling is reduced only for MgO but not for BaO. With an aim to understand the role of these additives and its improvement in cell performance, we have used microscopy, spectroscopy, ion beam analysis and diffraction based techniques to study the process. Transmission electron microscopy (TEM), and energy dispersive X-ray spectroscopy analysis (EDS) results showed evidence of crystalline MnO_2 particles for MgO as additive, whereas, MnO_2 particles with diffused structure leading to mixture of phases is observed for BaO additives which is in agreement with X-ray diffraction (XRD) data. This work relates to improvement in the electrochemical behaviour of the Zn–MnO_2 battery while the MgO additive helps to reduce the formation of manganese and zinc such as hetaerolite that hinders the lithium intercalation.

1. Introduction

Manganese dioxide (MnO_2) has been intensively investigated as promising electrode (cathode) material in a battery system [1,2] and electrochemical super capacitors [3,4] due to its excellent physical and chemical properties. The attractive features for implementing MnO_2 based material for battery application is the cost, non-toxicity and also an abundant transition metal. Hence, MnO_2 type batteries are attractive for energy storage applications i.e. electric vehicles that require plenty of materials in the current market. Today, MnO_2 as a cathode is used in alkaline primary as well as secondary batteries [5]. An alkaline battery has zinc (Zn) anode and manganese dioxide cathode with either potassium hydroxide or sodium hydroxide as an electrolyte. The Zn/MnO_2 battery is now well developed [6]. All the available literature [7–10] on alkaline cells is pertained to the proton insertion mechanism into MnO_2. We reported that when MnO_2 is discharged in cells containing aqueous lithium hydroxide (LiOH) electrolyte the mechanism appeared to be very different i.e. instead of proton (H^+) insertion, reversible lithium (Li^+) intercalation–deintercalation occurs into the host MnO_2. This resulted in opening up a new field of rechargeable batteries using aqueous solutions. Further to this, we demonstrated that good rechargeability could be obtained by suppressing the non-rechargeable discharged products like MnOOH, Mn_2O_3 and Mn_3O_4 while adding small amounts of additives into the MnO_2 cathode [11–13]. These manganese oxides and hydroxides compounds are detected because of the alkaline (LiOH) media.

In a recent paper [14] we reported an electrochemical behaviour into the effect of alkaline-earth oxide additions to the MnO_2 cathode with LiOH as the electrolyte. We found that the initial discharge capacity is improved for both the magnesium oxide (MgO) and barium oxide (BaO) additives but the capacity fade on multiple cycling is reduced only for MgO. In this paper, the mechanism involved on the battery performance is extensively investigated with an aims to (a) understand the role of MgO or BaO additives by comparing the electrochemical results with those of the previously published data [14] and (b) examine the electrode reactions of the initially discharged and multiple discharged cathode using X-ray diffraction (XRD), ion beam (elastic recoil detection) analysis, transmission electron microscopy (TEM) associated with energy dispersive (EDS) analysis.

* Corresponding author. Tel.: +61 8 9360 6784; fax: +61 8 9360 6343.
E-mail addresses: minakshi@murdoch.edu.au, lithiumbattery@hotmail.com (M. Minakshi).

0925-8388/$ – see front matter © 2011 Elsevier B.V. All rights reserved.
doi:10.1016/j.jallcom.2011.03.044

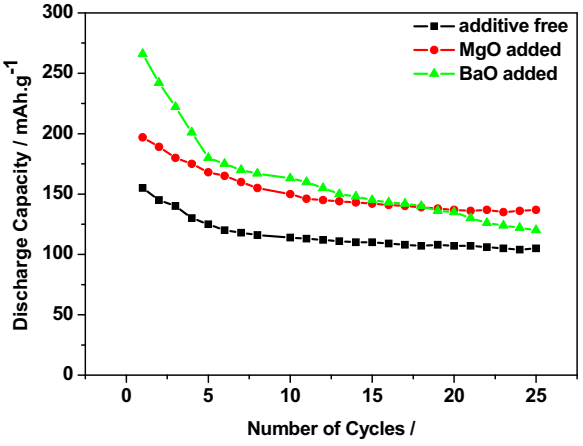

Fig. 1. Zn–MnO_2 battery using LiOH electrolyte illustrating the cycling profile of manganese dioxide (MnO_2) cathode containing (a) additive-free (b) MgO and (c) BaO 2 wt.% additives. An improved cell capacity is observed for MgO and BaO additions to the MnO_2 cathode. The capacity of the cell decreases quickly on cycling for BaO additive and approaches the capacity similar to that of additive free cathode.

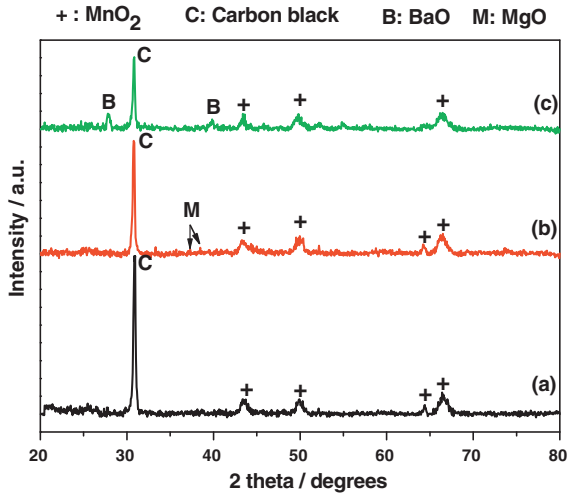

Fig. 2. XRD pattern of the manganese dioxide (MnO_2) cathode containing (a) additive-free (b) MgO and (c) BaO 2 wt.% additives before discharge.

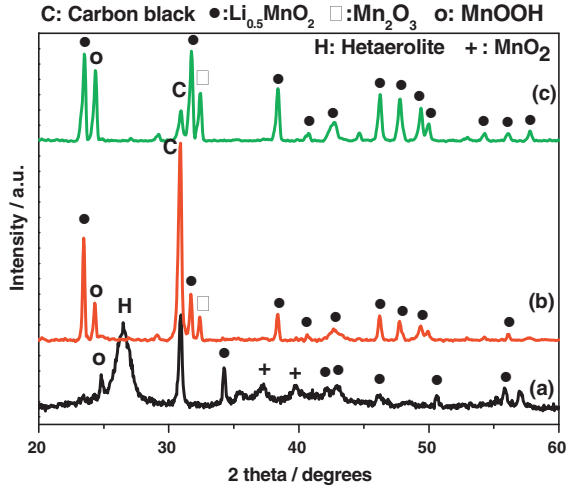

Fig. 3. XRD pattern of the discharged manganese dioxide (MnO_2) cathode containing (a) additive-free (b) MgO and (c) BaO 2 wt.% additives.

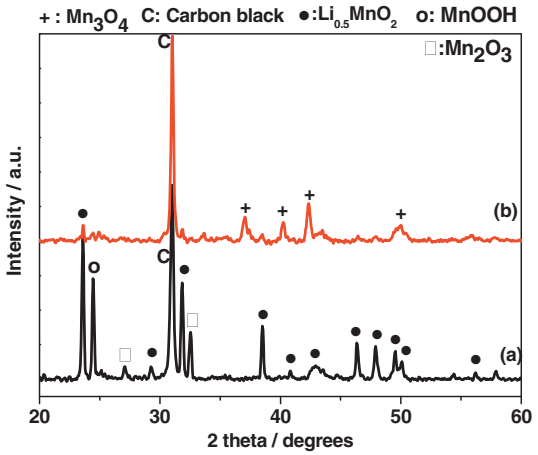

Fig. 4. XRD pattern of the multiple discharged manganese dioxide (MnO_2) cathode containing (a) MgO and (b) BaO 2 wt.% additives.

2. Experimental

The cell design, experimental details, and the method for preparing cathode samples have been described elsewhere [14]. The EMD (electrolytic manganese dioxide; γ-MnO_2) type (IBA sample 32) material used in this work was purchased from the Kerr McGee Chemical Corporation. Alkaline earth oxides i.e. magnesium oxide and barium oxide were obtained from Sigma–Aldrich. The cathode has been prepared from MnO_2 by physical admixture of at least one of the alkaline-earth oxides such as magnesium oxide or barium oxide. A cathode structure for an aqueous secondary battery comprise 73 wt.% MnO_2, 15 wt.% acetylene black as conductive powder, 10 wt.% poly (vinylidene difluoride) (PVDF, Sigma–Aldrich) as binder and 2 wt.% alkaline-earth oxide additive material uniformly mixed in a mortar and pestle and pressed to form a disk-like pellet. The pellet is 8 mm diameter and 0.5 mm

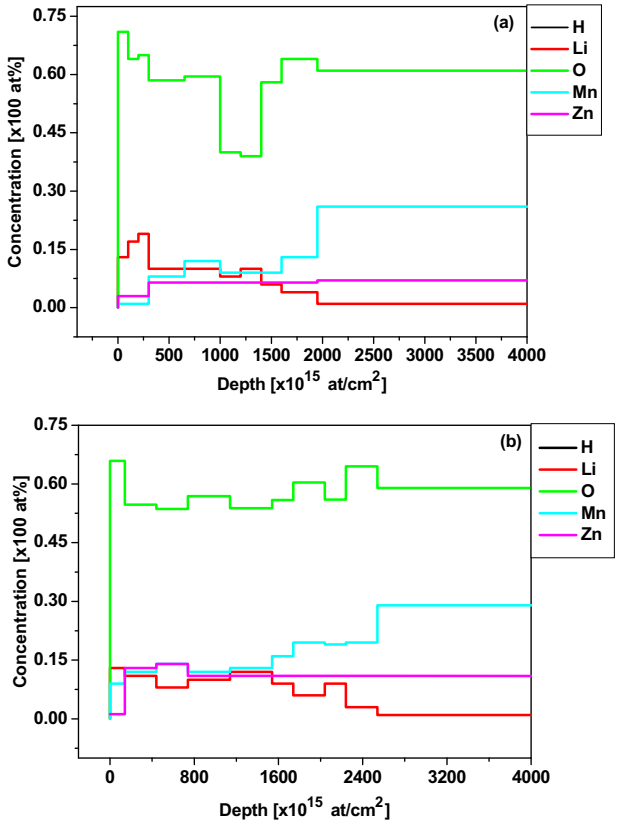

Fig. 5. ERDA spectrum of the elemental concentration of the multiple discharged manganese dioxide (MnO_2) cathode containing (a) MgO and (b) BaO 2 wt.% additives. The depth profile analysis (thickness in atoms/cm^2) of the elemental distribution is shown schematically.

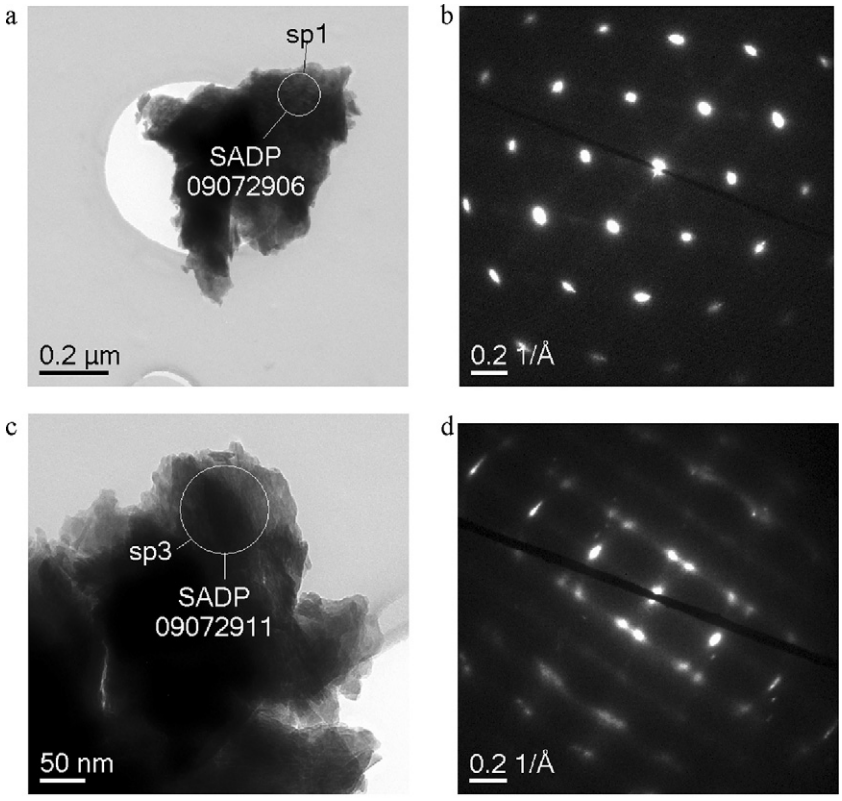

Fig. 6. TEM images and its selected area diffraction patterns (SADP) of the discharged MnO_2 for unmodified cathode. (a and b) initially discharged and (c and d) multiple discharged. Diffraction patterns in Fig. 6(b–d) are crystalline and diffusive, respectively, implying the presence of amorphous manganese oxy hydroxides compounds upon cycling.

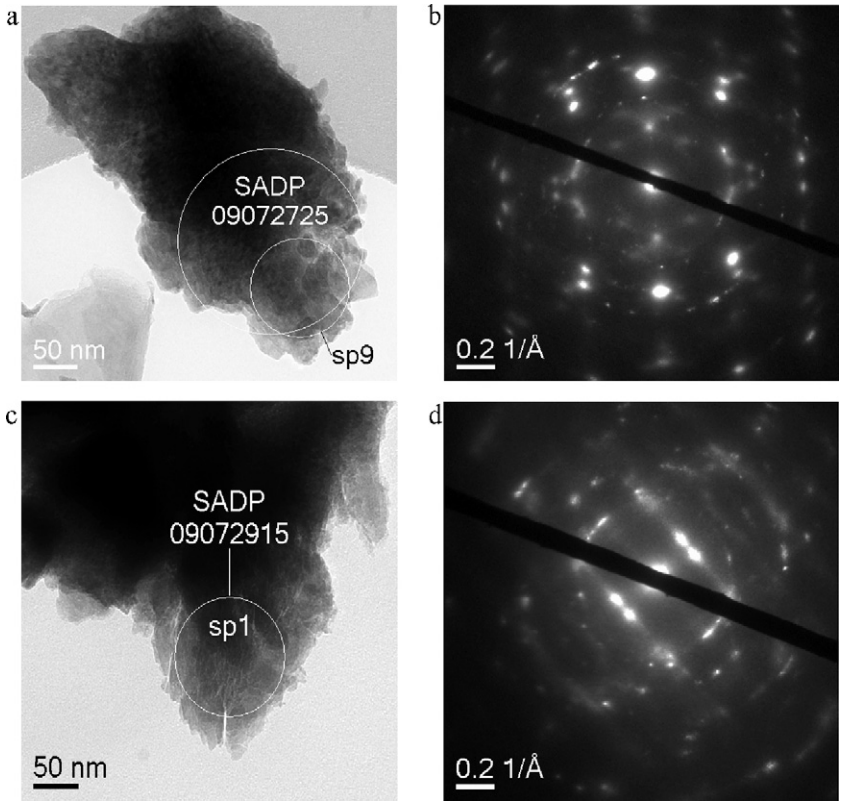

Fig. 7. TEM images and its selected area diffraction patterns (SADP) of the discharged MnO_2 for MgO (2 wt.%) modified cathode. (a and b) initially discharged and (c and d) multiple discharged. Diffraction patterns in Fig. 7(b–d) are identical implying the structure is versatile for reversibility.

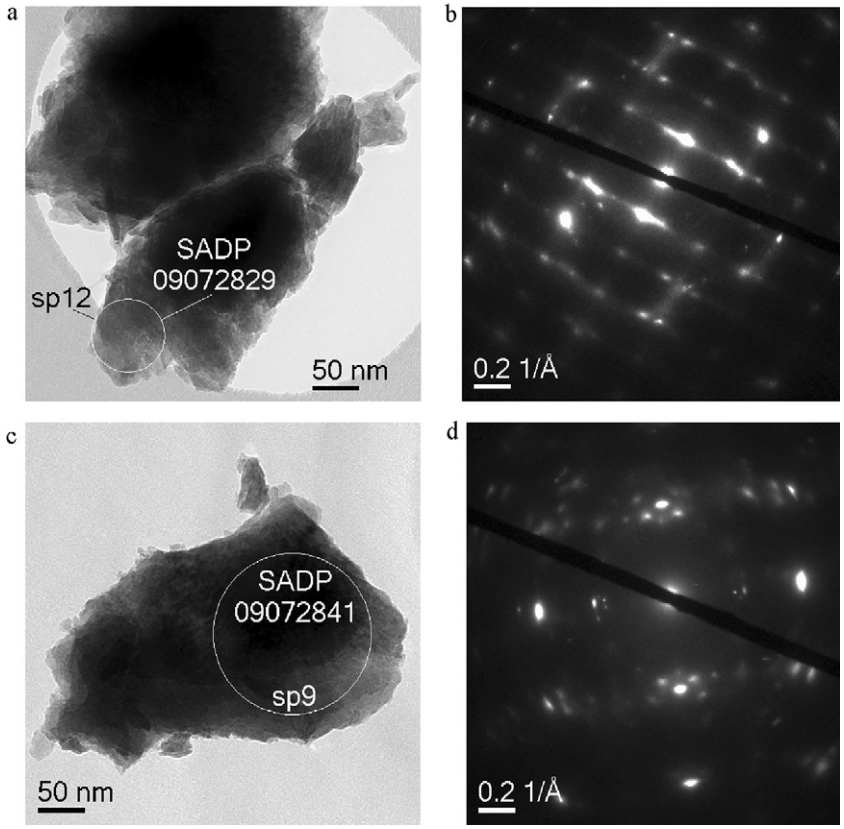

Fig. 8. TEM images and its selected area diffraction patterns (SADP) of the discharged MnO_2 for BaO (2 wt.%) modified cathode. (a and b) initially discharged and (c and d) multiple discharged. Diffraction patterns in Fig. 8(b–d) are not identical implying the structure is not reversible.

thickness. The electrolyte was a saturated solution of lithium hydroxide containing 1 mol L^{-1} zinc sulphate ($ZnSO_4$) with a pH equivalent of 10.5.

The morphology and interplanar spacings of the products formed for discharged MnO_2 samples were characterized by transmission electron microscopy, associated with energy dispersive spectra using a JEOL 2010F TEM model operated at 200 kV. TEM specimens were prepared by grinding a small fragment scraped from the pressed pellet under methanol and dispersing on a holey carbon support film. Specimens were examined at liquid nitrogen temperature in a cooling stage, to reduce beam damage and contamination effects. For X-ray analysis a Siemens D500 X-ray diffractometer 5635 using Co-Kα radiation was used. The voltage and current were 30 kV and 40 mA. The scan rate was 1°/min. Two theta values were recorded between 20° and 80°. Elemental concentrations of the MgO and BaO modified MnO_2 samples were quantified through the elastically forward scattered recoil atoms of the sample. This technique is referred to as elastic recoil detection analysis (ERDA). For ERDA analysis, the studies were performed on a 10 MV tandem ion beam accelerator using a 35 MeV Cl^{5+} ion beam with re-coiled particles being detected at 45°. The forward-recoiled atoms were mass analysed using a time-of-flight detection system. Both the TEM and ERDA experiments were conducted using the facilities of the Australian Nuclear Science and Technology Organisation (ANSTO), Australia.

3. Results and discussions

The influence of alkaline-earth oxide additives on the galvanostatic discharge–charge behaviour of the manganese dioxide cathode in a Zn–MnO_2 battery using lithium hydroxide as an electrolyte is reported in one of our earlier publication [14]. The cycling behaviour of manganese dioxide cathode in the presence of 2 wt.% magnesium oxide or barium oxide additive has been investigated here and compared (in Fig. 1) with additive free MnO_2. The MgO or BaO added MnO_2 was found to result in significantly improved initial discharge capacity of 196 and 265 mAh/g, respectively, compared to the additive free cell which shows just 145 mAh/g. However, the capacity of the BaO added cell decreases quickly (to 106 mAh/g) upon cycling and approached the value similar to that of additive free cathode after 25 cycles. Interestingly, the MgO added cell retains the cyclability to 140 mAh/g after 25 cycles and improved the cell capacity to 25%. This demonstrates that alkaline-earth oxides have influences on the electrochemical behaviour of the MnO_2 cathode but not in a similar mechanism that observed for a range of other additives (TiB_2 [11]; TiS_2 [12], Bi_2O_3 [13]) in that the formation of non-electroactive forms of manganese (MnOOH, Mn_2O_3 and Mn_3O_4) are suppressed. Surprisingly, in the alkaline earth oxide modified cathodes, the XRD patterns of the discharged product showed these non-electroactive forms of manganese still exist, as discussed in the following section.

Figs. 2–4 show X-ray diffraction patterns of the alkaline earth oxide modified MnO_2 cathodes before and after discharge, and after multiple cycles. The before discharge material (Fig. 2) shows the characteristic peaks of MnO_2, MgO and BaO as quoted in the JCPDS database, respectively (44-0143; 45-0946; 26-177). The main Bragg reflection corresponding to graphite (acetylene black) is seen at $2\theta = 30°$ (C). The XRD pattern of the discharged MnO_2 for additive free cathode (in Fig. 3a) is similar to that reported earlier [13] with a formation of hetaerolite ($ZnO.Mn_2O_3$) [15]. The alkaline earth oxide modified discharged cathode (Fig. 3b and c) shows the emergence of new peaks (◯, □ and ●). The original peaks of MnO_2 (+) are replaced by those of a number of new phases whereas the peak corresponding to C (graphite) is almost unchanged. As indexed in the XRD pattern these new reflections are in good agreement with those reported in the JCPDS database for the following materials: Mn_2O_3 (□), MnOOH (◯) and $Li_{0.5}MnO_2$ (●) i.e. lithium intercalated MnO_2. This shows that during discharge, manganese is (in part) reduced to various oxyhydroxides and lithium is also intercalated into the MnO_2 structure to form Li_xMnO_2. The peaks corresponding to the new phases in the BaO modified discharged cathode

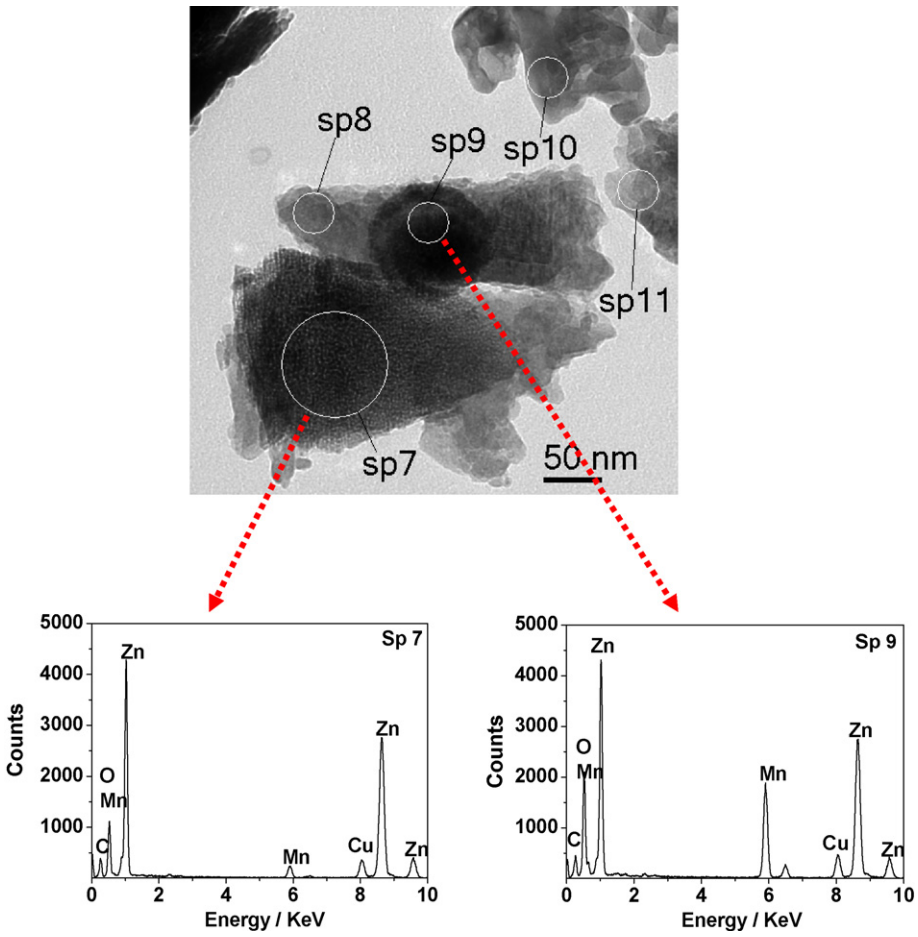

Fig. 9. Bright field image and its energy dispersive analysis (EDS) of the multiple discharged MnO_2 for BaO (2 wt.%) modified cathode. Bright field image showing clustered Zn area (sp 7) and Zn associated with MnO_2 areas (sp 8–11) (term "sp" refers to spectra). The EDS spectra of locations sp 7 and sp 9, elements are shown in the figure. The high peak intensity of Zn and Mn refers there is a formation of zincate ions in the BaO added MnO_2 cathode.

(Fig. 3c) is higher in intensity indicating that the manganese is reduced to a larger extent, resulting in higher discharge capacity, as evidenced in the cycling behaviour (Fig. 1). The presence of manganese oxides and hydroxides as the secondary compounds in the discharged product indicates that the role of alkaline earth oxide additives did not suppress the non-electro active compounds and it behaved differently from our previously investigated additives [11–13]. The XRD pattern for the multiple cycles of the MgO modified cathode material (Fig. 4a) is quite similar to that of the initial discharged cycle (Fig. 3b) indicating that the structure is reversible. The Li_xMnO_2 peaks were very similar suggesting that lithium insertion mechanism is reversible in the electrochemical process. However, peaks corresponding to manganese oxides and hydroxides i.e. non-rechargeable products were increased in peak intensity on multiple cycles thus resulting in a small fade in capacity (in Fig. 1). These secondary compounds are well known to be electrochemically inactive. Interestingly, for multiple cycles of the BaO modified MnO_2 cathode (Fig. 4b) a major reflections corresponding to Li_xMnO_2 (●) and MnOOH (○) are not present. However, a reflection corresponding to Mn_3O_4 (+) can be observed. The absence of Mn^{3+} (MnOOH and Mn_2O_3) in the XRD pattern suggests that the BaO addition does prevent the dissolution of Mn^{3+} from the solid MnO_2. The XRD diffraction pattern of the BaO added cell revealed differences in the discharged product obtained during initial (Fig. 3c) and multiple cycles (Fig. 4b). To confirm the presence of lithium in the cathode elastic recoil detection analysis was performed on the multiple discharged cathodes. ERDA analysis for the MgO modified cathode (Fig. 5a) confirmed the presence of lithium and its concentration was higher than that observed for BaO modified cathode (Fig. 5b) implying MgO is more reversible. Further, to better understand the role of these additives in MnO_2 and its mechanism, morphology and lattice imaging of the discharged cathode material were extensively investigated by TEM and its associated techniques.

The TEM image of the initial and multiple discharged MnO_2 for additive free cathode is shown in Fig. 6a and c. The bright field image showed the initial discharged MnO_2 to be crystalline and after multiple cycles a diffusive pattern is observed. The corresponding selected area diffraction pattern (SADP) showed a crystalline like pattern with bright spots (in Fig. 6b) for initial cycles while with a diffused pattern (in Fig. 6d) for multiple cycles supporting the bright field images. Hence, the resultant discharged product consists of mixed phases like crystalline Li_xMnO_2 and amorphous manganese oxides and hydroxides. The TEM images of the MgO modified MnO_2 particles after multiple cycles (in Fig. 7c) were similar to those in the initial discharged state (in Fig. 7a). The corresponding selected area diffraction (SADP in Fig. 7b–d) yielded spacings consistent with lithium intercalated MnO_2. This supports the XRD results that the product obtained upon discharge is reversible. Bright field imaging of the BaO modified MnO_2 particles after the first discharge cycle showed them to be highly crystalline (in Fig. 8a). However, the corresponding selected area diffraction pattern of the initial (in Fig. 8b) and multiple discharged cathodes (in Fig. 8d) distinguishes the variations between them. The MnO_2 was poorly crystalline, resulting in diffuse diffraction features after multiple cycles (as seen in Fig. 8c and d). This indicates that the structure is not reversible, hence

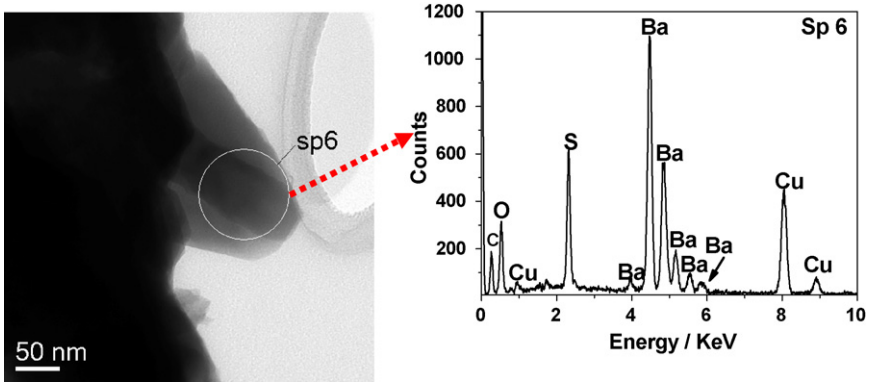

Fig. 10. Bright field image and its energy dispersive analysis (EDS) of the multiple discharged MnO_2 for BaO (2 wt.%) modified cathode. Bright field image showing clustered Ba rich area (sp 6) (term "sp" refers to spectra). The EDS spectra of location sp 6, elements are shown in the figure. The presence of peaks corresponding to Ba and S refers that barium is associated with sulphate suggesting that BaO may be reduced to $BaSO_4$ – that allows the zincate ions to reach the MnO_2 cathode.

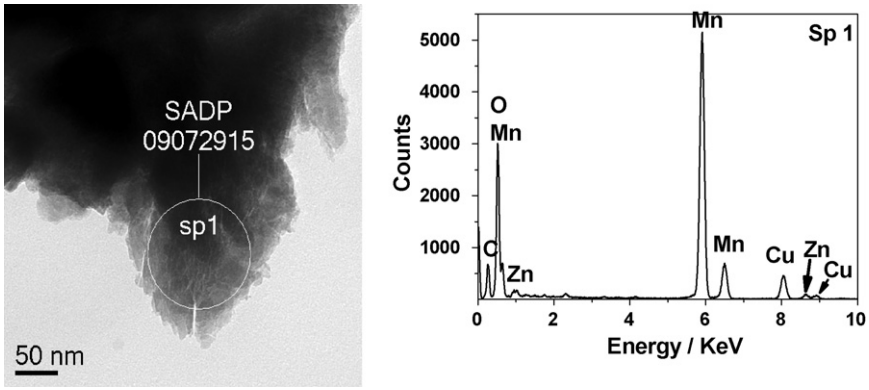

Fig. 11. Bright field image and its energy dispersive analysis (EDS) of the multiple discharged MnO_2 for MgO (2 wt.%) modified cathode. Bright field image showing clustered Mn rich area (sp 1) (term "sp" refers to spectra). The EDS spectra of location sp 1, elements are shown in the figure. The absence of peaks corresponding to Zn and S suggests there is no formation of zincate or sulphate ions. Hence the presence of MgO blocks the zincate ions to reach the MnO_2 cathode.

the loss in discharge capacity for BaO modified cathode. Now the question is why MgO more reversible than BaO additive? In order to elucidate the role of barium oxide in the LiOH electrolyte, the discharged cathode was characterised using TEM associated with EDS technique. Bright field TEM image for the BaO modified MnO_2 cathode after the multiple discharge cycle is shown in Fig. 9. The general morphology of the MnO_2 cluster is similar to the original material but individual crystals appear to be like spongy. The corresponding EDS spectra of this spongy region (Spectra "Sp" 7) show regions of polycrystalline zinc oxide in the vicinity of the MnO_2 cathode. EDS spectra recorded from the Zn region associated with MnO_2 (Sp 9) invariably contained small amounts of zincate ions, which is from the Zn anode. In another region of labelled (Sp 6 in Fig. 10) shows barium rich area is associated with sulphate suggesting barium oxide is reduced to barium sulphate over time in the LiOH electrolyte. This allows the formation of zincate ions near the MnO_2 cathode forming a byproduct double oxide of manganese and zinc such as hetaerolite ($ZnO.Mn_2O_3$ or $ZnMn_2O_4$) [15–17]. Such a byproduct of discharge reaction lowers electron conductivity of MnO_2 electrode causing an increase in its internal resistance while hindering intercalation mechanism thereby causing an increase in concentration polarization. The elemental depth profile analysis (Fig. 5b) showed Zn concentration is higher in the cathode. This result in a capacity fade as observed for BaO modified cathode in Fig. 1. The bright field imaging of the MgO modified MnO_2 cathode after multiple discharge is shown in Fig. 11. The corresponding EDS analysis in the region labelled Sp 1, does not show any evidence for the formation of zincate or sulphate ions, supporting the ERDA analysis in Fig. 5a. This suggests MgO additive blocks the zincate ions into the region of MnO_2 cathode thereby the formation of hetaerolite is prevented. This enhances the cyclability of the MgO modified cathode in Fig. 1. Therefore, addition of alkaline earth oxides leads to a better utilization of MnO_2 cathode, nevertheless MgO behaves differently from BaO in terms of cycleability.

Based upon these results, it can be concluded that the performance of MgO additive is superior to the range of other additives (TiB_2 [11]; TiS_2 [12], Bi_2O_3 [13]; B_4C or B_4N [18]; CeO_2 [19]) investigated for MnO_2 cathode. This could be explained in terms of the nature of MgO, which has a unique characteristic, like acting as a binder to fuse the MnO_2 grains and helps in reducing the porosity [20]. Hence, an optimum MgO content (2 wt.%) in the MnO_2 cell improves its rechargeability.

4. Conclusions

The electrochemical behaviour reported here showed the effect of alkaline earth oxide additions to MnO_2 enhanced the performance of the Zn–MnO_2 battery. The addition of 2 wt.% MgO or BaO additives to MnO_2 resulted in a significantly higher discharge capacity. The barium oxide additive reduced to barium sulphate over time in the LiOH electrolyte, which allowed the formation of zincate ions from Zn anode in the vicinity of the MnO_2 cathode thereby forming the by-product hetaerolite ($ZnO.Mn_2O_3$ or $ZnMn_2O_4$). The discharged product of the MgO modified MnO_2 characterized by TEM showed that MgO helps to reduce the formation of hetaerolite while improving the reversibility of the lithium

intercalation-de intercalation process. The formation of hetaerolite deteriorated the host MnO_2 structure resulting in a capacity fade for unmodified and BaO modified cathode.

Acknowledgements

The author (M.M) wishes to acknowledge the Australian Research Council (ARC). This research was supported under Australian Research Council's Discovery Projects funding scheme (DP1092543). M.M would like to thank the Australian Institute of Nuclear Science and Engineering (AINSE) for providing financial assistance (AINGRA Award 10053) for access to TEM and ERDA facilities at ANSTO.

References

[1] M. Sugantha, P.A. Ramakrishnan, A.M. Hermann, C.P. Warmsingh, D.S. Ginley, Int. J. Hydrogen Energy 28 (2003) 597.
[2] S. Bach, J.P. Pereira-Ramos, N. Baffier, R. Messina, Electrochim. Acta 36 (1991) 1595.
[3] M. Toupin, T. Brousse, D. Bélanger, Chem. Mater. 16 (2004) 3184.
[4] V. Subramanian, H.W. Zhu, R. Vajtai, P.M. Ajayan, B.Q. Wei, J. Phys. Chem. B 109 (2005) 20207.
[5] K. Kordesch, J. Gsellmann, J. Electranal. Chem. Interfacial Electrochem. 118 (1981) 187.
[6] G. Leclanche, L. Monde, C. R. Acad. Sci. 83 (1876) 54 (16 (1868) 532).
[7] J.M. Amarilla, F. Tedjar, C. Poinsignon, Electrochim. Acta 39 (1994) 2321.
[8] Y. Chabre, J. Pannetier, Prog. Solid State Chem. 23 (1995) 1.
[9] S. Bach, S. Beliar, C. Cachet-Vivier, J.P. Pereira-Ramos, L. Sanchez, P. Lavela, J.L. Tirado, Electrochim. Acta 45 (1999) 931.
[10] H.S. Wroblowa, N. Gupta, J. Electroanal. Chem. 238 (1987) 93.
[11] M. Minakshi, D.R.G. Mitchell, P. Singh, Electrochim. Acta 52 (2007) 3294.
[12] M. Minakshi, D.R.G. Mitchell, K. Prince, Solid State Ionics 179 (2008) 355.
[13] M. Minakshi, D.R.G. Mitchell, Electrochim. Acta 53 (2008) 6323.
[14] M. Minakshi, Ind. Eng. Chem. Res., submitted for publication.
[15] M. Kloβ, D. Rahner, W. Plieth, J. Power Sources 69 (1997) 137.
[16] C.L. Shope, Y. Xie, C.H. Gammons, Appl. Geochem. 21 (2006) 476.
[17] F. Jean, C. Cachet, L.T. Yu, J. Appl. Electrochem. 27 (1997) 635.
[18] M. Minakshi, M. Blackford, G. Thorogood, T.B. Issa, Electrochim. Acta 55 (2010) 1028.
[19] M. Minakshi, K. Nallathamby, D.R.G. Mitchell, J. Alloys Compd. 479 (2009) 87.
[20] W.C. Li, A.H. Lu, C. Weidenthaler, F. Schuth, Chem. Mater. 16 (2004) 5676.